Turing-like instabilities from a limit cycle

Joseph D. Challenger,[1,2] Raffaella Burioni,[3] and Duccio Fanelli[2]
[1]*Department of Infectious Disease Epidemiology, Imperial College London, London, W2 1PG, United Kingdom*
[2]*Dipartimento di Fisica e Astronomia, Università di Firenze, INFN and CSDC, Via Sansone 1, 50019 Sesto Fiorentino, Firenze, Italy*
[3]*Dipartimento di Fisica e Scienza della Terra and INFN, Università di Parma, viale G. P. Usberti 7/A 43124, Parma, Italy*
(Received 7 March 2015; published 26 August 2015)

The Turing instability is a paradigmatic route to pattern formation in reaction-diffusion systems. Following a diffusion-driven instability, homogeneous fixed points can become unstable when subject to external perturbation. As a consequence, the system evolves towards a stationary, nonhomogeneous attractor. Stable patterns can be also obtained via oscillation quenching of an initially synchronous state of diffusively coupled oscillators. In the literature this is known as the oscillation death phenomenon. Here, we show that oscillation death is nothing but a Turing instability for the first return map of the system in its synchronous periodic state. In particular, we obtain a set of approximated closed conditions for identifying the domain in the parameter space that yields the instability. This is a natural generalization of the original Turing relations, to the case where the homogeneous solution of the examined system is a periodic function of time. The obtained framework applies to systems embedded in continuum space, as well as those defined on a networklike support. The predictive ability of the theory is tested numerically, using different reaction schemes.

DOI: 10.1103/PhysRevE.92.022818 PACS number(s): 89.75.Fb, 89.75.Kd, 05.45.Xt

I. INTRODUCTION

From chemistry to physics, passing through biology and ecology, patterns are widespread in nature. Under specific conditions, the spontaneous drive to self-organization which acts on an ensemble of interacting constituents materializes in a rich zoology of beautiful motifs, that bear intriguing universal traits [1–12]. The spirals that originate from chemical reactions, the stripes in fish skin patterning, the feline coat coloration, and the spatial patterns in dryland vegetation are all examples of the intrinsic ability of seemingly different systems to yield regular structures, both in space and time.

In 1952, Turing wrote a seminal paper [13] on the theory of morphogenesis, establishing the mathematical principles that drive the process of pattern formation. To this end, he considered the coupled evolution of two spatially distributed species, subject to microscopic reactions and freely diffusing in the embedding medium. Working in this context, Turing proved that a homogeneous mean-field solution of the examined reaction diffusion system can be unstable to external perturbations. The Turing instability, as the effect is nowadays called, is seeded by diffusion and requires an activator-inhibitor scheme of interaction between agents [14]. When the conditions for the instability are met, the perturbation grows exponentially in the linear regime. The system subsequently evolves towards an asymptotic stationary stable solution characterized by a patchy, spatially inhomogeneous, density distribution, which indirectly reflects the collection of modes made unstable at short time and the geometry of the hosting support [15]. Traveling waves can also set in following a symmetry-breaking instability of a homogeneous fixed point.

Turing instabilities are classically studied on regular lattices or continuous supports. For a large class of problems, however, the inspected system is defined on a complex network. The theory of patterns formation extends to this latter case, as discussed in the pioneering paper by Othmer and Scriven [16], and recently revisited by Nakao and Mikhailov [17]. Reaction-diffusion systems defined on a graph can produce an effective segregation into activator-rich and activator-poor nodes, Turing-like patterns on a heterogeneous spatial support.

In the classical Turing paradigm, the conditions for the onset of the instability are derived via a linear stability analysis, which requires expanding the imposed perturbation on the complete basis formed by the eigenvectors of the (continuum or discrete) Laplacian [17,18]. Compact inequalities, containing the entries of the Jacobian matrix for the linearized problem and the diffusion constants for the interacting species, are then derived which constitute the necessary condition for the instability to develop [15].

The formation of a nonuniform stationary state has also been observed in the dynamics of diffusively coupled oscillators. Weak coupling of nonlinear oscillators leads to synchronization, a fundamental phenomenon in nonlinear dynamics which plays a pivotal role in many branches of science. Oscillation quenching is an interesting related phenomenon, which is seen in spatially coupled systems [19]. Indeed, the possibility of disrupting the oscillations could be in principle exploited as an efficient dynamical regulator [20,21]. Moreover, it could be implicated in pathological neuronal drive, as in the Alzheimer and Parkinson diseases. Two different types of oscillation quenching phenomena are generally distinguished in the literature, which differ both in the fundamental mechanisms of generation, as well as in their respective manifestations. The suppression of the oscillations can yield a final homogeneous steady state, a dynamical process that is known as amplitude death. Oscillation death (OD) is instead observed when the initially synchronized state evolves towards an asymptotic, inhomogeneous configuration [22–24], in response to an externally imposed perturbation [19]. As remarked upon in the literature (see, e.g., Ref. [22]), the OD pathway is reminiscent of the Turing symmetry-breaking transition, which, as we here recall, originally assumes a reaction-diffusion system perturbed around a homogeneous, time-independent, equilibrium. Amplitude and

oscillation death have also been studied on complex networks, but less work has been done in this direction (see, e.g., Refs. [25,26]).

Models exhibiting amplitude or oscillation death are, however, difficult to investigate. To progress in the analysis it is customary to invoke a normal form representation for the amplitude of the unstable modes near a Hopf bifurcation. Less attention has been devoted to inspecting multispecies reaction-diffusion systems, for which the analysis proves more cumbersome. Alternatively, the master stability formalism [27] can be employed to determine the stability (via the largest Floquet exponent [28]) of the synchronous state, at a given coupling strength.

Building on these concepts, the aim of this paper is to shed further light on the analogy between OD and Turing instability and eventually base it on solid, quantitative grounds. As we shall prove in the following, OD is nothing but a Turing instability for the first return map of the system in its synchronous periodic state. Arguing along these lines, we will develop an approximation scheme in order to obtain a set of closed conditions for identifying the domain in the parameter space that yields the sought instability. Such conditions constitute an obvious generalization of Turing original relations, to the interesting setting where the homogeneous solution of the examined system is a periodic function of time. The usual Turing inequalities, which are exact, are recovered when the limit cycle collapses to a fixed point, thus revealing a generalized picture which is consistent with the classical paradigm for pattern formation. The obtained framework holds both for systems embedded in continuum space as well as for those defined on a complex network. The predictive ability of the theory will be demonstrated for different reaction schemes, and we will discuss the accuracy of the theory in different circumstances.

The paper is organized as follows. In the next section, we shall review the fundamentals of the Turing instability theory. Then, we will move on to studying the effect of a tiny heterogeneous perturbation acting on a collection of synchronous reaction-diffusion oscillators. In Sec. III we will make use of the master stability function approach, complemented by standard Floquet analysis. Then, in Sec. IV we will derive the generalized Turing conditions to which we alluded above. Numerical simulations are reported in Sec. V (for the Brusselator and Schnakenberg models) to illustrate the characteristics of the patterns that are asymptotically attained. Here, we shall consider the systems defined on a two-dimensional continuum domain, subject to periodic boundary conditions, as well as on a heterogeneous network of the Watts-Strogatz type. In this section we will also test the accuracy of the generalized Turing conditions against the Floquet-based results. Finally, in Sec. VI we sum up and draw our conclusions.

II. BASIC THEORY OF THE TURING INSTABILITY

Consider the following reaction-diffusion system:

$$\begin{aligned}\frac{\partial \phi}{\partial t} &= f(\phi,\psi) + D_\phi \nabla^2 \phi,\\ \frac{\partial \psi}{\partial t} &= g(\phi,\psi) + D_\psi \nabla^2 \phi,\end{aligned} \tag{1}$$

where $\phi(\mathbf{r},t)$ and $\psi(\mathbf{r},t)$ denote the concentration of the interacting species of respective diffusion constants D_ϕ and D_ψ. The position in space is specified by the vector $\mathbf{r}$ and t stands for time; $f(\ldots,\ldots)$ and $g(\ldots,\ldots)$ are nonlinear functions of the concentrations and represent the reaction contributions. We assume that a stable homogeneous fixed point exists, so that $\phi(\mathbf{r}) = \bar{\phi}$ and $\psi(\mathbf{r}) = \bar{\psi}$, with $\bar{\phi}$ and $\bar{\psi}$ constants, such that $f(\bar{\phi},\bar{\psi}) = g(\bar{\phi},\bar{\psi}) = 0$. To formally verify the stability of the fixed point, we introduce the Jacobian matrix $\mathbf{J}$:

$$\mathbf{J} = \begin{pmatrix} f_\phi & f_\psi \\ g_\phi & g_\psi \end{pmatrix}. \tag{2}$$

Here, f_ϕ stands for the derivative of f with respect to the density ϕ evaluated at the fixed point $(\bar{\phi},\bar{\psi})$. Similar considerations hold for f_ψ, g_ϕ, g_ψ. The homogeneous fixed point is stable provided that

$$\mathrm{tr}(\mathbf{J}) = f_\phi + g_\psi < 0, \tag{3}$$

$$\det(\mathbf{J}) = f_\phi g_\psi - f_\psi g_\phi > 0, \tag{4}$$

where tr(...) and det(...) denote, respectively, the trace and the determinant. The Turing approach consists of introducing a small perturbation $\mathbf{w}$ of the initial homogeneous stationary state and looking for the conditions that eventually yield to the growth of such disturbance. In formulas, we set

$$\mathbf{w} = \begin{pmatrix} \delta\phi \\ \delta\psi \end{pmatrix} \equiv \begin{pmatrix} \phi - \bar{\phi} \\ \psi - \bar{\psi} \end{pmatrix}. \tag{5}$$

By hypothesis $|\mathbf{w}|$ is small, so we can linearize system (1) around the fixed point to eventually obtain

$$\dot{\mathbf{w}} = \mathbf{J}\mathbf{w} + \mathbf{D}\nabla^2\mathbf{w}, \tag{6}$$

where $\dot{\mathbf{w}}$ represents the time derivative of $\mathbf{w}$ and $\mathbf{D}$ is the diagonal diffusion matrix:

$$\mathbf{D} = \begin{pmatrix} D_\phi & 0 \\ 0 & D_\psi \end{pmatrix}. \tag{7}$$

To solve the above system subject to specific boundary conditions one can introduce the eigenfunctions $\mathbf{W}_k(\mathbf{r})$ of the Laplacian as

$$-\nabla^2\mathbf{W}_k(\mathbf{r}) = k^2\mathbf{W}_k(\mathbf{r}), \tag{8}$$

for all $k \in \sigma$, where σ is a suitable (unbounded) spectral set. We can then expand the perturbation $\mathbf{w}$ as

$$\mathbf{w}(\mathbf{r},t) = \sum_{k\in\sigma} c_k e^{\lambda(k)t}\mathbf{W}_k(\mathbf{r}), \tag{9}$$

where the constants c_k are determined by the initial condition. This operation is equivalent to performing a Fourier transform in space of the original linearized equations. The complex function $\lambda(k)$, also known as the dispersion relation, controls the growth or damping of the initial perturbation. The solution of the linearized system exists provided that

$$\det[\lambda I - \mathbf{J}(k^2)] = 0, \tag{10}$$

where I is the 2×2 identity matrix and $\mathbf{J}(k^2)$ is the modified Jacobian matrix with the inclusion of the spatial components,

namely,

$$\mathbf{J}(k^2) = \begin{pmatrix} f_\phi - D_\phi k^2 & f_\psi \\ g_\phi & g_\psi - D_\psi k^2 \end{pmatrix}. \tag{11}$$

From Eq. (9) one obtains the characteristic polynomial

$$\lambda^2 - B\lambda + C = 0, \tag{12}$$

where

$$\begin{aligned} B &= f_\phi + g_\psi - (D_\phi + D_\psi)k^2, \\ C &= D_\phi D_\psi k^4 - (D_\phi g_\psi + D_\psi f_\phi)k^2 + f_\phi g_\psi - f_\psi g_\phi. \end{aligned} \tag{13}$$

Since we are interested in the growth of the unstable perturbation, we should select the largest $\lambda(k) \equiv \lambda_{\max}$ which can be written as

$$\lambda_{\max} = \tfrac{1}{2}(B + \sqrt{B^2 - 4C}). \tag{14}$$

Recalling that, by hypothesis, $\mathrm{tr}[\mathbf{J}(0)] < 0$, one can immediately conclude that $B < 0$ for all k. Hence, the condition of the instability $\lambda_{\max} > 0$ translates into $C < 0$. To obtain a set of closed analytical conditions for the instability, we observe that C is a convex parabola in k^2. The minimum of the parabola is located at

$$k^2_{\min} = \frac{(D_\phi g_\psi + D_\psi f_\phi)}{2D_\phi D_\psi}, \tag{15}$$

and the corresponding value of C, hereafter called $C^{\min}$, reads as

$$C^{\min} = -\frac{(D_\phi g_\psi + D_\psi f_\phi)^2}{4(D_\phi D_\psi)^2} + f_\phi g_\psi - f_\psi g_\phi. \tag{16}$$

By imposing $C^{\min} < 0$ and requiring for consistency reasons $k^2_{\min} > 0$ yields the following conditions for the instability to develop:

$$\begin{aligned} &(D_\phi g_\psi + D_\psi f_\phi)^2 > 4D_\phi D_\psi (f_\phi g_\psi - f_\psi g_\phi), \\ &(D_\phi g_\psi + D_\psi f_\phi) > 0. \end{aligned} \tag{17}$$

The above inequalities, complemented with the additional conditions (3), are routinely applied to determine the parameter choice that makes a reaction-diffusion model unstable to externally imposed perturbation of the homogeneous fixed point. Starting from this point, we shall obtain a straightforward generalization of the classical Turing picture, which includes the oscillation death pathway as one of its possible manifestations.

Before concluding this section, we remark that the above analysis can be readily adapted to the case of a system defined on a network of N nodes. A concise description of this translation can be found in the Appendix.

III. LINEAR INSTABILITY ANALYSIS AROUND A PERIODIC TIME-DEPENDENT SOLUTION: THE FLOQUET APPROACH

In this section, we consider the evolution of an external perturbation on an ensemble of synchronous oscillators. Our starting point is again system (1) which we now imagine to admit a homogeneous stable solution $(\bar\phi(t), \bar\psi(t))$, which is periodic with period T. We therefore require $\bar\phi(t+T) = \bar\phi(t)$ and $\bar\psi(t+T) = \bar\psi(t)$, for all time t. In general the curve $\bar{\mathbf{x}}(t) \equiv (\bar\phi(t), \bar\psi(t))$ cannot be calculated in closed form, but it can be determined numerically with a prescribed level of accuracy.

Before proceeding, one must check the stability of the limit-cycle solution. This fact can be assessed via a direct application of Floquet theory [28], that we will here describe. We begin by focusing on a simplified problem, found by ignoring the spatial components of system (1). In other words, we will commence by studying the uniform counterpart of system (1), where the concentrations are solely dependent on time.

We consider a dynamical path starting close to, but not on, the limit cycle. If the limit cycle is stable, the difference between this path, here called $\mathbf{x}(t)$, and the limit cycle $\bar{\mathbf{x}}(t)$ should decay, as time progresses. Introduce $\xi(t) = \mathbf{x}(t) - \bar{\mathbf{x}}(t)$, by definition small, and linearize the governing equations to obtain

$$\dot\xi = \mathbf{J}(t)\xi, \tag{18}$$

where the Jacobian matrix is now evaluated at the limit cycle and depends therefore on time. Due to the periodic nature of $\bar{\mathbf{x}}(t)$, all elements of $\mathbf{J}(t)$ are periodic and the Floquet theory is hence applicable. Let us label with $\mathbf{X}(t)$ a fundamental matrix of system (18). Then, for all t, there exists a singular, constant matrix $\mathbf{B}$ such that [28]

$$\mathbf{X}(t+T) = \mathbf{X}(t)\mathbf{B}. \tag{19}$$

In addition, the following relation holds:

$$\det\mathbf{B} = \exp\left[\int_0^T tr\mathbf{J}(t)dt\right]. \tag{20}$$

The matrix B depends in general on the choice of the fundamental matrix $\mathbf{X}(t)$ employed. Nevertheless, its eigenvalues, and hence determinant, do not. The eigenvalues ρ_1 and ρ_2 of $\mathbf{B}$ are usually called the Floquet multipliers of the linearized system (18). One can also introduce the corresponding Floquet exponent μ_i defined via the implicit relation $\rho_i = \exp(\mu_i T)$, for $i = 1,2$. If ρ is a characteristic multiplier for (18) and μ the associated exponent, a particular solution of (18) has the form [28]

$$\xi(t) = e^{\mu t}\mathbf{p}(t), \tag{21}$$

where $\mathbf{p}(t)$ is a periodic function of period T, i.e., such that $\mathbf{p}(t+T) = \mathbf{p}(t)$. General solutions of the two-dimensional system (18) can be therefore cast in the form

$$\xi(t) = c_1 e^{\mu_1 t}\mathbf{p}^{(1)} + c_2 e^{\mu_2 t}\mathbf{p}^{(2)}, \tag{22}$$

where the constants c_1 and c_2 are determined by the initial conditions. For all linear expansions about limit cycles arising from first-order equations, one of the Floquet exponents of the system vanishes ($\mu_1 = 0$ or, equivalently, $\rho_1 = 1$) throughout the limit-cycle phase.[1] The remaining exponent μ_2 assumes negative real values. The zero exponent is associated with

[1]The nonlinear system being considered admits a periodic solution, the limit cycle, which we called $\bar{\mathbf{x}}(t)$. One can easily show that $d\bar{\mathbf{x}}(t)/dt$ is a solution of the linearized problem (18). Since $d\bar{\mathbf{x}}(t)/dt$ is also a periodic function of period T, then the general solution (22) implies that one of Floquet multipliers, say ρ_1, must be equal to unity or, equivalently, $\mu_1 = 0$.

perturbations along the longitudinal direction of the limit cycle: these perturbations are neither amplified nor damped as the motion progresses. At variance, perturbations in the transverse direction decay in time if the limit cycle is stable. Recalling that $\det\mathbf{B} = \rho_1\rho_2$, for a stable limit cycle one has $\det\mathbf{B} = \rho_2 = \exp(\mu_2 T) < 1$ and therefore

$$\int_0^T \mathrm{tr}\mathbf{J}(t)dt = \int_0^T [f_\phi(t) + g_\psi(t)]dt < 0, \tag{23}$$

a relation that will prove useful in the following.

Let us now return to discussing the original problem at hand. Assume the reaction-diffusion system to be initialized in the region of the parameters that yields a stable limit-cycle behavior. Therefore, the concentration depends on time, in a periodic fashion. In addition, we assume a uniform spatial distribution, meaning that the oscillators are initially synchronized, with no relative dephasing. We then apply a small, nonhomogeneous (thus site-dependent) perturbation and ask ourselves if the interplay between reaction and diffusion can drive the system towards a spontaneous symmetry breaking instability. This is nothing but the oscillation death phenomenon that we here discuss in the framework of a self-consistent reaction-diffusion framework.

To answer the question, one can adapt to the scope the Floquet analysis outlined above, considering the generalized linear equation (18), with the inclusion of space. More concretely, Eq. (18) reads as

$$\dot{\xi} = \mathbf{J}(k^2,t)\xi. \tag{24}$$

The matrix $\mathbf{J}(k^2,t)$ is formally given by (11), and its entries are evaluated at the stable (aspatial) limit cycle $\bar{\mathbf{x}}(t)$. Floquet theory ensures the existence of a solution of problem (24) in the form (22) where now μ_1 and μ_2 depend explicitly on the spatial index k. If $\mu_{\max}$, the largest of the μ_i, takes positive values over a bounded window in k, the reaction-diffusion system is unstable to the imposed perturbation. The latter grows exponentially in time, and progressively disrupts the synchrony of the initial configuration. The largest Floquet exponent $\mu_{\max}$ is the analog of the dispersion relation $\lambda_{\max}$ for the Turing instability and ultimately sets the route to the phenomenon of oscillation death. Unfortunately, the determination of $\mu_{\max}$ follows a purely numerical approach and, at this stage, the similarity between Turing and oscillation death cannot be explored in detail.

In the next section, we shall discuss an alternative, approximate, approach to the study of the instability of a perturbed array of synchronous oscillators. We will derive clear perturbative conditions for the onset of the instability, which will allow us to reconcile the Turing paradigm and the oscillation death phenomenon, under a unifying framework.

IV. ALTERNATIVE CONDITIONS FOR THE DIFFUSION-DRIVEN INSTABILITY OF A UNIFORM LIMIT-CYCLE SOLUTION

We now turn to derive an alternative criterion to identify the region of diffusion-driven instability from a uniform limit-cycle condition. Our predictions will be then confronted to those obtained following the canonical approach based on the Floquet theory. Let us start from the linearized equation (24) and imagine to partition the interval $[0,T]$ into a collection of M contiguous sub-intervals $[t_i,t_{i+1}]$. We assume that M is sufficiently large that the width of each subinterval $\Delta t = t_{i+1} - t_i$ can be assumed small. To simplify the reasoning we have assumed a uniform partition, but this is not a necessary requirement for the following derivation to hold.

The idea is to solve the linear equation (24) within each (small) window of time duration Δt, and then use this knowledge to estimate the cumulative growth of the perturbation, over one complete loop of the limit cycle. In practical terms, and as already anticipated in the Introduction, we will look at the stability of the first return map, which is associated to the periodic limit-cycle solution of the inspected reaction diffusion kinetics. Inside each subinterval, the perturbation ξ obeys a linear ordinary differential equation with time-dependent coefficients.

Such an equation can be approximated using a forward Euler scheme, so to establish a direct link between $\xi_{i+1} \equiv \xi(t_{i+1})$ and $\xi_i \equiv \xi(t_i)$:

$$\xi_{i+1} = [I + \Delta t\mathbf{J}(k^2,t_i)]\xi_i + O(\Delta t^2). \tag{25}$$

To compute the global evolution of the perturbation along the limit cycle, one needs to calculate

$$\xi_M = \Pi_{j=0}^{M-1}[I + \Delta t\mathbf{J}(k^2,t_j)]\xi_0. \tag{26}$$

Here, one must note that, because a product of matrices is not in general commutative, the terms in the product must be "time ordered," with the earlier times to the right. Neglecting the terms which scale as Δt^n with $n \geqslant 2$, in agreement with the approximated expression (25), yields

$$\xi_M \simeq \left[I + \Delta t\sum_j \mathbf{J}(k^2,t_j)\right]\xi_0. \tag{27}$$

In the limit $\Delta t \to 0$ (which implies sending simultaneously $M \to \infty$), one can replace the above sum with an integral and write the mapping from ξ_0 to ξ_M as

$$\xi(T) = \left[I + \int_0^T \mathbf{J}(k^2,t)dt\right]\xi_0 \simeq \exp\left(\int_0^T \mathbf{J}(k^2,t)dt\right)\xi_0. \tag{28}$$

Higher order corrections can be also estimated by replacing the Euler scheme (26) with a refined multistep approximation of the Runge-Kutta type and performing a similar algebraic manipulation of the equations involved. We leave this extension to future work and present instead a different derivation of the above result, which yields consistent conclusions.

In fact, a formal solution of Eq. (18) can be written as

$$\xi_{i+1} = \exp[\mathbf{\Omega}(t_{i+1},t_i)]\xi_i, \tag{29}$$

where $\mathbf{\Omega}(t_{i+1},t_i) = \sum_{k=1}^{\infty}\mathbf{\Omega}_{k,i}$. The form of the first few $\mathbf{\Omega}_{k,i}$ elements are

$$\begin{aligned}
\mathbf{\Omega}_{1,i} &= \int_{t_i}^{t_{i+1}} \mathbf{J}(k^2,\tau_1)d\tau_1,\\
\mathbf{\Omega}_{2,i} &= \frac{1}{2}\int_{t_i}^{t_{i+1}} d\tau_1 \int_{t_i}^{\tau_1} d\tau_2[\mathbf{J}(k^2,\tau_1),\mathbf{J}(k^2,\tau_2)],\\
\mathbf{\Omega}_{3,i} &= \frac{1}{6}\int_{t_i}^{t_{i+1}} d\tau_1 \int_{t_i}^{\tau_1} d\tau_2 \int_{t_i}^{\tau_3} d\tau_3
\end{aligned} \tag{30}$$

$$\times [\mathbf{J}(k^2,\tau_1),[\mathbf{J}(k^2,\tau_2),\mathbf{J}(k^2,\tau_3)]]$$
$$+[[\mathbf{J}(k^2,\tau_3),\mathbf{J}(k^2,\tau_2)],\mathbf{J}(k^2,\tau_1)],$$

where $[\ldots,\ldots]$ stands for the matrix commutator. The above solution is also known as the Magnus series expansion [29]. From the definition of the coefficients (30), it follows that $\mathbf{\Omega}_{s,i} \simeq O([\Delta t]^s)$. Since, by assumption, Δt is small, one can truncate the infinite sum in the explicit solution (29). In particular, we will consider explicitly the leading term in the series expansion, to quantify the dominant contribution. Upon truncation, we have therefore

$$\xi_{i+1} \simeq \exp(\Omega_{1,i})\xi_i. \tag{31}$$

Making use of the above relation, we can for instance relate ξ_2 to ξ_0 as

$$\xi_2 = \exp(\mathbf{\Omega}_{1,1})\xi_1 = \exp(\mathbf{\Omega}_{1,1})\exp(\mathbf{\Omega}_{1,0})\xi_0. \tag{32}$$

To progress in the analysis we first recall the Baker-Campbell-Hausdorff formula. Consider two noncommuting matrices $\mathbf{Z_1}$ and $\mathbf{Z_2}$. Then, the product $\exp(\mathbf{Z_1})\exp(\mathbf{Z_2})$ can be written as $\exp(\mathbf{Z})$ where

$$\mathbf{Z} = \mathbf{Z_1} + \mathbf{Z_2} + \tfrac{1}{2}[\mathbf{Z_1},\mathbf{Z_2}] + \ldots, \tag{33}$$

where $[\ldots,\ldots]$ stands for the matrix commutator. If matrices $\mathbf{Z_1}$ and $\mathbf{Z_2}$ commute, namely if $[\mathbf{Z_1},\mathbf{Z_2}] = 0$, one recovers the usual formula for the composition of the exponential of scalars. Making use of the above relation in the expression (32) for ξ_2, one obtains

$$\xi_2 = \exp\left(\mathbf{\Omega}_{1,1} + \mathbf{\Omega}_{1,0} + \tfrac{1}{2}[\mathbf{\Omega}_{1,1},\mathbf{\Omega}_{1,0}] + \ldots\right)\xi_0. \tag{34}$$

The correlator $[\mathbf{\Omega}_{1,1},\mathbf{\Omega}_{1,0}]$ involves the product of terms of order $O(\Delta t^2)$, and it should be therefore neglected for consistency reasons, as the expansion is truncated at order $O(\Delta t)$. Moreover, it can be argued that the commutation of matrices defined on neighbor intervals of the partition in t scales as Δt^3, an observation that makes it cumbersome to organize the next to leading corrections in growing powers of Δt.

The reasoning that we have outlined above can be iterated forward. One gets eventually the following expression for the magnitude of the perturbation ξ_M, at the considered order of approximation:

$$\xi_M = \exp\left(\sum_{j=0}^{M-1} \Omega_{1j}\right)\xi_0. \tag{35}$$

Performing the continuum limit ($\Delta t \to 0$ and $M \to \infty$), we obtain

$$\xi(T) \simeq \exp\left[\int_0^T \mathbf{J}(k^2,\tau_1)d\tau_1\right]\xi(0) = \exp(\langle\mathbf{J}\rangle T)\xi_0, \tag{36}$$

where $\langle\mathbf{J}\rangle = (1/T)\int_0^T \mathbf{J}(k^2,\tau)d\tau$. The above equation coincides with Eq. (28), obtained under the Euler scheme.

Starting from this setting, it is possible to derive a compact criterion for the onset of the instability, which we will then validate *a posteriori* versus the standard Floquet technique. To this end, we assume $\langle\mathbf{J}\rangle$ to be diagonalizable. Hence, there exist a matrix $\mathbf{U}$ such that $\langle\mathbf{J}\rangle = \mathbf{U}\mathbf{D}_J\mathbf{U}^{-1}$ where $\mathbf{D}_J$ is a diagonal matrix. Equation (36) transforms into

$$\xi(T) = \exp(\mathbf{U}\mathbf{D}_J\mathbf{U}^{-1}T)\xi(0) = \mathbf{U}\exp(\mathbf{D}_J T)\mathbf{U}^{-1}\xi(0). \tag{37}$$

We now introduce $\eta = \mathbf{U}^{-1}\xi$. The map (36) then takes the simple form

$$\eta(T) = \exp(\mathbf{D}_J T)\eta(0). \tag{38}$$

The eigenvalues of the averaged Jacobian matrix $\mathbf{J}$ determine the fate of the perturbation. If the real part of the largest eigenvalue is positive, then the perturbation develops, otherwise it fades away after successive iteration of the return map. To derive the condition for the emergence of the instability one must therefore calculate the eigenvalues $\lambda_{1,2}$ of $\langle\mathbf{J}\rangle$, which are the solutions of the following characteristic polynomial:

$$\lambda^2 - B_{(1)}\lambda + C_{(1)} = 0, \tag{39}$$

where

$$\begin{aligned} B_{(1)} &= \langle f_\phi\rangle + \langle g_\psi\rangle - (D_\phi + D_\psi)k^2, \\ C_{(1)} &= D_\phi D_\psi k^4 - (D_\phi\langle g_\psi\rangle + D_\psi\langle f_\phi\rangle)k^2 \\ &\quad + \langle f_\phi\rangle\langle g_\psi\rangle - \langle f_\psi\rangle\langle g_\phi\rangle, \end{aligned} \tag{40}$$

where $\langle f_\phi\rangle = (1/T)\int_0^T f_\phi dt$. Similarly, for $\langle f_\psi\rangle$, $\langle g_\phi\rangle$, and $\langle g_\psi\rangle$. Hence, the largest real eigenvalue $\lambda_{\max}$ is

$$\lambda_{\max} = \tfrac{1}{2}\left(B_{(1)} + \sqrt{B_{(1)}^2 - 4C_{(1)}}\right). \tag{41}$$

Recalling that by definition $B_{(1)} < 0$ (the limit cycle is stable), the condition of the instability $\lambda_{\max} > 0$ translates into $C_{(1)} < 0$. This is nothing but the same condition that it is recovered following the conventional Turing calculation with the only difference that now the time-dependent entries of the Jacobian matrix are averaged over one complete loop of the unperturbed limit cycle. To obtain closed analytical condition for the instability, one can repeat the steps of the derivation reported in Sec. II to eventually get

$$\begin{aligned} &(D_\phi\langle g_\psi\rangle + D_\psi\langle f_\phi\rangle)^2 > 4D_\phi D_\psi(\langle f_\phi\rangle\langle g_\psi\rangle - \langle f_\psi\rangle\langle g_\phi\rangle), \\ &(D_\phi\langle g_\psi\rangle + D_\psi\langle f_\phi\rangle) > 0, \end{aligned} \tag{42}$$

which constitute a natural generalization of the standard Turing recipe. Indeed, the above relations reduce to the Turing conditions when the limit cycle converges to a fixed point. The appendix of this article describes how the above analysis can easily be generalized to the case where the system is defined on a complex network. In the next section, we will present some numerical results, including an examination of the accuracy of the approximation scheme outlined above.

V. NUMERICAL VALIDATION

To test the adequacy of the theory, we shall consider two distinct reaction schemes: the Brusselator and the Schnakenberg model. For both systems, we will delimit the portion of the relevant parameters space for which the instability is expected to develop, based on conditions (42). These predictions are compared to those obtained using Floquet analysis. Numerical simulations are also performed to challenge the validity of the proposed theoretical picture.

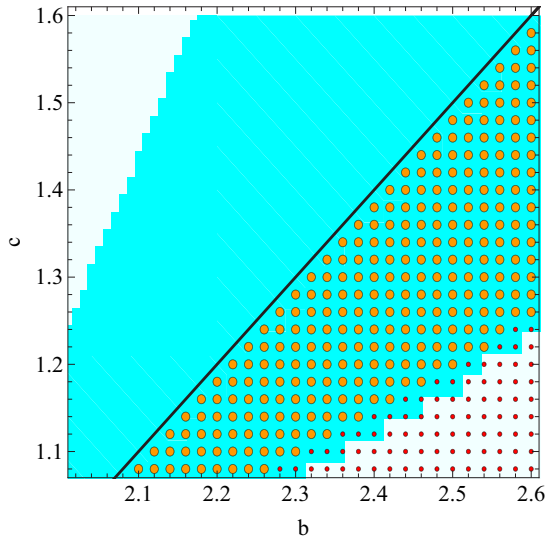

FIG. 1. (Color online) The extended region of the Turing instability for the Brusselator model, as parameters b and c are varied. The diffusion coefficients were $D_\phi = 0.07$, $D_\psi = 0.5$. The solid line shows the Hopf bifurcation for the aspatial model: above the line the aspatial system converges toward a stable fixed point. Below the line, a stable homogeneous limit-cycle solution is instead found. The circular symbols show results from the Floquet approach: the larger symbols indicating an instability, the smaller ones indicating that the homogeneous system is stable. The shaded region identifies the region of parameter space where the instability is predicted to occur, following Eq. (42).

A. Brusselator model

Here, we will make use of the so-called Brusselator model, a two species reaction-diffusion model whose local reaction terms are $f(\phi,\psi) = 1 - (b+1)\phi + c\phi^2\psi$ and $g(\phi,\psi) = b\psi - c\phi^2\psi$, where b and c act as control parameters. Conditions (42) allow us to delimit a compact portion of the parameter plane (b,c) for which the generalized Turing instability is expected to develop. Results of the study are reported in Fig. 1: the solid line separates the fixed point from the limit-cycle regime. The region of instability, the shaded area in the figure, extends beyond the Hopf bifurcation, and includes the standard Turing domain as part of it. As discussed earlier, the instability domain inside the region of stable homogeneous limit cycle can be calculated via a direct implementation of the Floquet technique. Large orange circles in Fig. 1 identify the instability domain as computed via the Floquet analysis, while small red dots refer to the choice of the parameters for which the OD instability cannot take place. These results agree with the prediction obtained from the generalized Turing inequalities (42). In Fig. 2, we show the dispersion relations for three parameter choices. Fixing $b = 2.5$, we vary the value of c, showing results from inside and outside the instability region.

Numerical simulations are also performed for the system initialized inside the extended region of instability to visualize the asymptotic, stationary stable solution that the system eventually attains. To emphasize the broad relevance of our conclusion, we performed simulations for (i) the Brusselator model defined on a regular two-dimensional support, subject to periodic boundary conditions (see Fig. 3); (ii) the Brusselator model defined on a Watts-Strogatz network [30] (see Fig. 4).

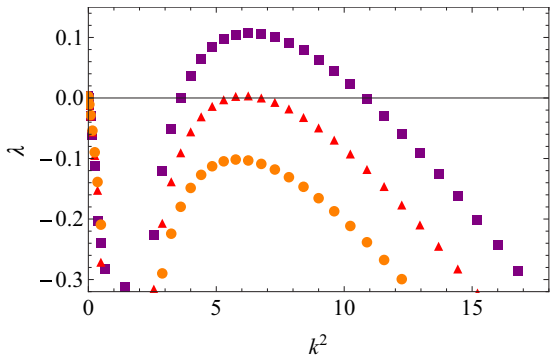

FIG. 2. (Color online) Dispersion relations for the Brusselator model for three parameter choices, calculated from the Floquet analysis. Fixing $b = 2.5$, we used $c = 1.3$ (purple squares), $c = 1.2$ (red triangles), and $c = 1.1$ (orange circles). The diffusion coefficients were $D_\phi = 0.07$, $D_\psi = 0.5$.

We also used the Brusselator model to look at the accuracy of the approximation scheme, presented in the previous section. In particular, we wish to compare the results for the full numerical integration, found using Eq. (26) evaluated over one period of the limit cycle, and the approximate result found in Eq. (36). In each case, $\xi(T)$ is found by applying a matrix operator, say Γ, to $\xi(0)$. In Appendix B, Figs. 9 and 10 compare the four elements of Γ in the case where $k = 0$, for two choices of the reaction parameters. We find that, both in this instance and in general, that the approximation is very accurate when the limit cycle is small (which is the case near to the Hopf bifurcation), but loses accuracy as the limit cycle becomes larger, although the general trend of Γ versus k^2 is still captured. We believe that this is due to more significant

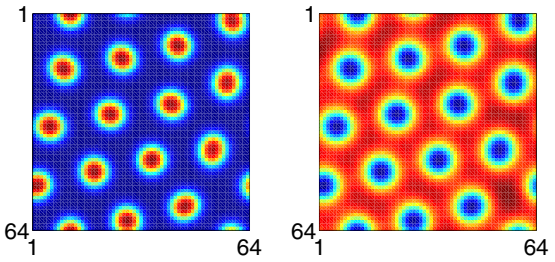

FIG. 3. (Color online) The late time evolution for species ϕ (left) and ψ (right) for the Brusselator model inside the extended region of Turing-like order. The initial homogeneous limit-cycle state is disturbed by a small nonhomogeneous perturbation. The synchrony of the spatially coupled oscillators is lost and the system evolves towards a stationary stable configuration. The patterns resemble (indeed, under the Fourier lens, are identical to) the patterns obtained inside the classical Turing region, i.e., above the Hopf transition line. In other words, it looks like the same Turing attractor can be reached following two alternative dynamical pathways. Parameters are $b = 2.4$; $c = 1.2$; $D_\phi = 0.07$, $D_\psi = 0.5$. The simulations are carried our over a square box of linear size $L = 10$ partitioned in 64 mesh points.

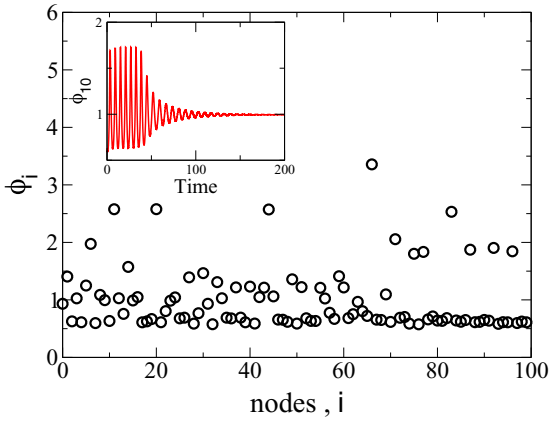

FIG. 4. (Color online) Stationary pattern attained by the Brusselator model, defined on a network of the Watts-Strogatz type (number of node $N = 100$ and probability of rewiring $p = 0.8$). In the main panel, the asymptotic concentration of species ϕ_i is plotted as function of the nodes index i. In the inset, the evolution of the concentration on a particular node is shown, in order to appreciate the transition from the initial oscillatory regime to the final stationary state. The parameters are set as in Fig. 3.

contributions from the matrix commutators in the Magnus expansion, given in Eq. (30).

B. Schnakenberg model

We shall here consider the Schnakenberg model [31] and repeat the analysis reported above. The Schnakenberg model is

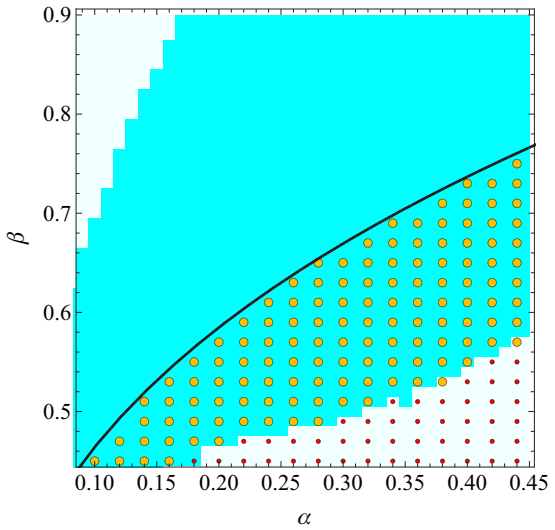

FIG. 5. (Color online) The extended region of the Turing instability for the Schnakenberg model, as parameters α and β are varied. The diffusion coefficients were $D_\phi = 0.01$, $D_\psi = 1$. The solid line shows the Hopf bifurcation for the aspatial model: above the line the aspatial system converges toward a stable fixed point. Below the line, a stable homogeneous limit-cycle solution is instead found. The circular symbols show results from the Floquet approach: the larger symbols indicating an instability, the smaller ones indicating that the homogeneous system is stable. The shading delimits the region where the instability is predicted to occur by Eqs. (42).

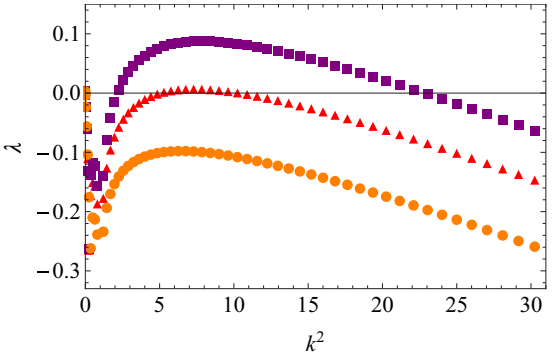

FIG. 6. (Color online) Dispersion relations for the Schnakenberg model for three parameter choices, calculated from the Floquet analysis. Fixing $\alpha = 0.36$, we used $\beta = 0.56$ (purple squares), $\beta = 0.52$ (red triangles), and $\beta = 0.48$ (orange circles). The diffusion coefficients were $D_\phi = 0.01$, $D_\psi = 1$.

characterized by the following reaction terms: $f(\phi,\psi) = a - \phi + \phi^2\psi$ and $g(\phi,\psi) = b - \phi^2\psi$, where a and b are constant parameters. A model of this form was used by Gierer and Meinhardt to study pattern formation [14]. Like Schnakenberg, we employ it as a model that exhibits limit-cycle behavior in the aspatial case. To study the system, it is customary to introduce the parameters $\alpha = b - a$ and $\beta = a + b$. The shaded area in Fig. 5 identifies the region of the parameter plane (α,β) where the instability is predicted to occur. We again emphasize that patterns are expected to occur outside the region of classical Turing order, well inside the domain where the aspatial models display a stable limit-cycle solution. As for the case of the Brusselator model, one reaches consistent conclusions if the Floquet analysis is employed instead of Eqs. (42), the generalized Turing inequalities. In Fig. 6, we show the dispersion relations for three parameter choices. Fixing $\alpha = 1.3$, we vary the value of β, showing results from inside and outside the instability region. Numerical simulations for the Schnakenberg system defined both on a

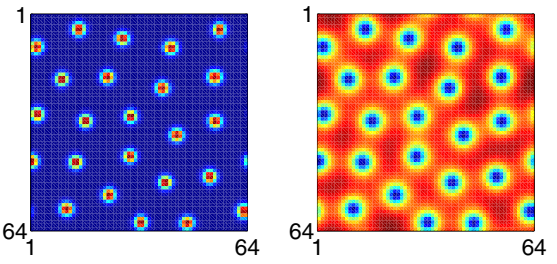

FIG. 7. (Color online) The final stationary state obtained for species ϕ by initializing the Schnakenberg model inside the region where the homogeneous (hence aspatial) limit cycle is stable, and imposing a small perturbation to the initially synchronous oscillations. As already remarked in the caption of Fig. 3, the patterns are practically indistinguishable from those obtained inside the classical Turing region. Here also, it seems plausible to hypothesize that the same Turing attractor can be reached following alternative dynamical paths. Parameters are $a = 0.125$, $b = 0.475$ (or $\alpha = 0.35$ and $\beta = 0.6$), $D_\phi = 0.01$, $D_\psi = 1$. The simulations are carried our over a square box of linear size $L = 10$ partitioned in 64 mesh points.

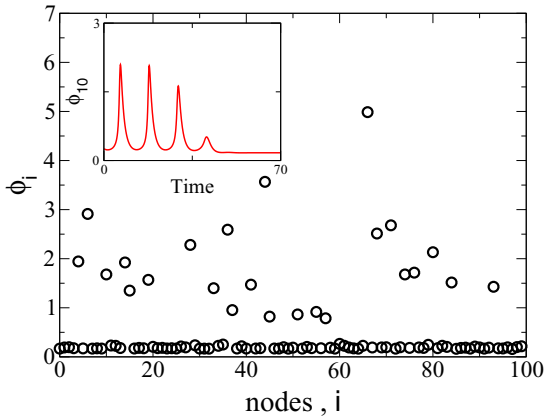

FIG. 8. (Color online) Stationary pattern attained by the Schnakenberg model, defined on a network of the Watts-Strogatz type (number of nodes $N = 100$ and probability of rewiring $p = 0.8$). In the main panel, the asymptotic concentration of species ϕ_i is plotted as function of the nodes index i. In the inset, the time evolution of the concentration on one of the nodes of the network is shown. The transition from the initial oscillation to the final stationary state is clearly displayed. The parameters are set as in Fig. 7.

continuous two-dimensional support and on a heterogeneous complex network are performed and the asymptotic, stationary stable patterns displayed in Figs. 7 and 8, respectively.

VI. CONCLUSION

Reaction-diffusion systems display a plethora of interesting solutions. Particularly relevant is the spontaneous emergence of self-organized stationary patterns, originating from a symmetry breaking instability of a homogeneous fixed point. The dynamical mechanism that seeds such an instability was illustrated by Turing in his pioneering work on the chemical basis of morphogenesis. Since then, it has been exploited in many different contexts, ranging from physics to biology. The concept of the Turing instability also applies to reaction-diffusion systems defined on a complex network, a setting that is of paramount importance for neuroscience-related applications. The internet and the cyberworld in general are other obvious examples which require the concept of network.

Beyond the Turing picture, stationary regular motifs can also originate from oscillation quenching of a spatially extended chain of coupled nonlinear oscillators. This phenomenon, usually referred to as oscillation death, has been mainly investigated by resorting to a normal form approximation for the evolution of the spatially unstable modes. Mathematical progress is possible via a semianalytical approach which combines knowledge from the celebrated master stability formalism [27] to the Floquet technique.

Starting from this setting, we have here investigated the process of pattern formation for a multispecies model, which displays a limit-cycle behavior in its aspatial limit. We have showed that oscillation death is nothing but the classical Turing instability for the first return map of the system in its synchronous periodic state. Working along these lines we have obtained a system of compact inequalities, which set the conditions for the onset of the instability. The obtained conditions constitute a natural generalization of the Turing recipe, so as to include the case where the imposed perturbation acts on a homogeneous time-dependent periodic solution. The proposed criterion returns a wider region of Turing instability, as compared to the conventional approach. The framework that we have established here can be easily applied to the case where the system is established on a complex network, which has relevance in many applications. The stationary patterns that originate from the inhomogeneous perturbation of the limit-cycle solution are virtually indistinguishable from those obtained within the classical Turing region, as we demonstrated with reference to specific case studies. Based on these findings, we propose that the conditions for the generalized instability that we have derived should be carefully considered for all reaction-diffusion schemes, which undergo Turing ordering while displaying a limit-cycle solution in their aspatial counterpart versions.

APPENDIX A: PROCEDURE ON A COMPLEX NETWORK

The purpose of this appendix is to briefly discuss the generalization of the above analysis to the relevant setting where the reaction-diffusion system is defined on a discrete support, such as a complex heterogeneous network.

We begin by considering a network made of N nodes and characterized by the $N \times N$ adjacency matrix W: the entry W_{ij} is equal to one if nodes i and j (with $i \neq j$) are connected, and it is zero otherwise. If the network is undirected, the matrix W is symmetric. A general reaction-diffusion system defined on the network reads as

$$\begin{aligned} \frac{d\phi_i}{dt} &= f(\phi_i,\psi_i) + D_\phi \sum_j \Delta_{ij}\phi_j, \\ \frac{d\psi_i}{dt} &= g(\phi_i,\psi_i) + D_\psi \sum_j \Delta_{ij}\psi_j. \end{aligned} \tag{A1}$$

Here, $\Delta_{ij} = W_{ij} - k_i\delta_{ij}$ is the network Laplacian, k_i stands for the connectivity of node i, and δ_{ij} is the Kronecker delta. Assume now that a homogeneous fixed point of system (A1) exists and indicate it with $(\bar{\phi},\bar{\psi})$. The fixed point is stable provided Eqs. (3) hold. Patterns arise when $(\bar{\phi},\bar{\psi})$ becomes unstable to inhomogeneous perturbations. As already discussed with reference to the continuum setting, one can introduce a small perturbation $(\delta\phi_i,\delta\psi_i)$ to the fixed point and linearize around it, to look for the conditions that seed the instability. One obtains a linear equation which is equivalent to Eq. (6) except for the index i which is attached to the perturbation amount, and hence to $\mathbf{w}$, and which reflects the discreteness of the embedding structure. To solve the linear problem, one needs to introduce the spectrum of the Laplacian operator

$$\sum_{j=1}^{N} \Delta_{ij} v_j^{(\alpha)} = \Lambda^{(\alpha)} v_i^{(\alpha)}, \quad \alpha = 1,\ldots,N \tag{A2}$$

where $\Lambda^{(\alpha)}$ and $v_i^{(\alpha)}$, respectively, represent the eigenvalues and their associated eigenvectors. Then, the inhomogeneous

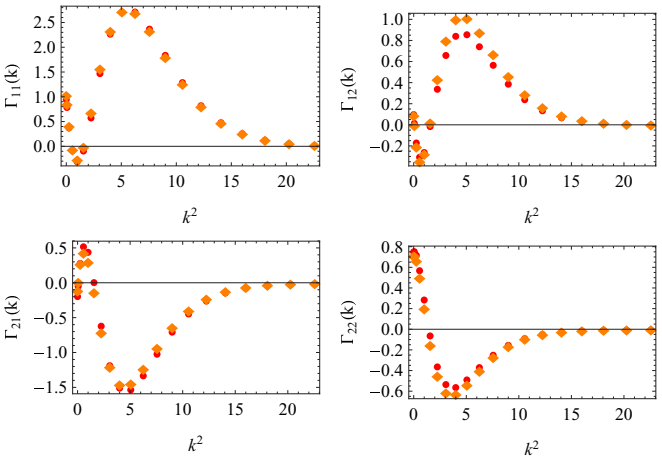

FIG. 9. (Color online) Comparison of the matrix operator Γ used in Eqs. (26) (orange diamonds) and (36) (red circles). Results were obtained from the Brusselator model with reaction parameters $c = 1.2$ and $b = 2.25$.

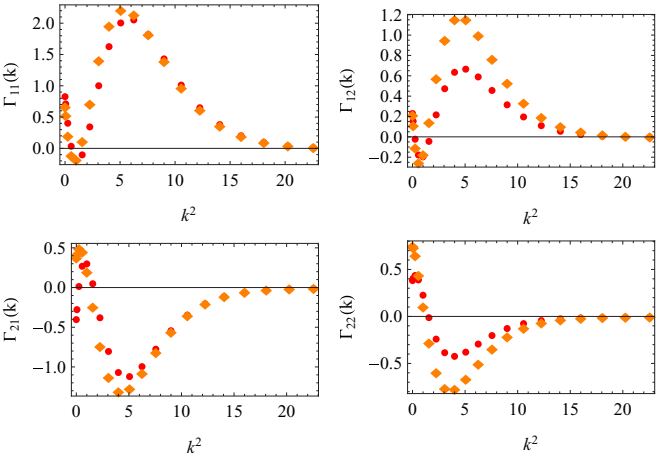

FIG. 10. (Color online) Comparison of the matrix operator Γ used in Eqs. (26) (orange diamonds) and (36) (red circles). Results were obtained from the Brusselator model with reaction parameters $c = 1.2$ and $b = 2.35$.

perturbation can be expanded as

$$\delta\phi_i = \sum_{j=1}^{N} c_\alpha e^{\lambda_\alpha t} v_i^{(\alpha)}, \tag{A3}$$

$$\delta\psi_i = \sum_{j=1}^{N} b_\alpha e^{\lambda_\alpha t} v_i^{(\alpha)}, \tag{A4}$$

where the constants c_α and b_α refer to the initial condition. By inserting the above expression in the equation which governs the evolution of the perturbation at the linear order, one gets a dispersion relation which is identical to (14), provided the factor $-k^2$ is replaced with the Laplacian eigenvalues $\Lambda^{(\alpha)}$.

In practice, it is this latter quantity which determines the spatial characteristic of the emerging patterns, when the system is defined on a heterogeneous complex support. Obviously, inequalities (42) extend to the case of networks, noting that $-k^2$ hands over into $\Lambda^{(\alpha)}$. The discussion above adapts easily to the case where the perturbation is studied around a homogeneous limit-cycle solution.

APPENDIX B: ASSESSING THE ACCURACY OF THE APPROXIMATION SCHEME

In this appendix, we check the accuracy of the approximation scheme used to find the generalized condition for the instability of the synchronized state. Figures 9 and 10 show results from the Brusselator model, for two choices of the parameters. Results are discussed in the main text.

[1] G. Nicolis and I. Prigogine, *Self-Organization in Non-Equilibrium Systems* (Wiley, New York, 1977).

[2] M. Mimura and J. D. Murray, On a diffusive prey-predator model which exhibits patchiness, J. Theor. Biol. **75**, 249 (1978).

[3] J. L. Maron and S. Harrison, Spatial pattern formation in an insect host-parasitoid system, Science **278**, 1619 (1997).

[4] M. Baurmann, T. Gross, and U. Feudel, Instabilities in spatially extended predator-prey systems: Spatio-temporal patterns in the neighborhood of Turing-Hopf bifurcations, J. Theor. Biol. **245**, 220 (2007).

[5] M. Rietkerk and J. van de Koppel, Regular pattern formation in real ecosystems, Trends Ecol. Evol. **23**, 169 (2008).

[6] H. Meinhardt and A. Gierer, Pattern formation by local self-activation and lateral inhibition, BioEssays **22**, 753 (2000).

[7] M. P. Harris, S. Williamson, J. F. Fallon, H. Meinhardt, and R. O. Prum, Molecular evidence for an activator-inhibitor mechanism in development of embryonic feather branching, Proc. Natl. Acad. Sci. USA **102**, 11734 (2005).

[8] P. K. Maini, R. E. Baker, and C-M. Chuong, The Turing model comes of molecular age, Science **314**, 1397 (2006).

[9] S. A. Newman and R. Bhat, Activator-inhibitor dynamics of vertebrate limb pattern formation, Birth Defects Res. (Part C) **81**, 305 (2007).

[10] T. Miura and K. Shiota, TGF β2 acts as an "activator" molecule in reaction-diffusion model and is involved in cell sorting phenomenon in mouse limb micromass culture, Dev. Dyn. **217**, 241 (2000).

[11] A. M. Zhabotinsky, M. Dolnik, and I. R. Epstein, Pattern formation arising from wave instability in a simple reaction-diffusion system, J. Chem. Phys. **103**, 10306 (1995).

[12] M. R. Ricard and S. Mischler, Turing instabilities at Hopf bifurcation, J. Nonlinear Sci. **19**, 467 (2009).

[13] A. M. Turing, The chemical basis of morphogenesis, Philos. Trans. R. Soc., B **237**, 37 (1952).

[14] A. Gierer and H. Meinhardt, A. theory of biological pattern formation, Kybernetik **12**, 30 (1972).

[15] J. D. Murray, *Mathematical Biology*, 2nd ed. (Springer, New York, 1991).

[16] H. G. Othmer and L. E. J. Scriven, Instability and dynamic pattern in cellular networks, J. Theor. Biol. **32**, 507 (1971);

Non-linear aspects of dynamic pattern in cellular networks, *ibid.* **43**, 83 (1974).

[17] H. Nakao and A. S. Mikhailov, Turing patterns in network-organized activator-inhibitor systems, Nat. Phys. **6**, 544 (2010).

[18] M. Asllani, J. D. Challenger, F. S. Pavone, L. Sacconi, and D. Fanelli, The theory of pattern formation on directed networks, Nat. Commun. **5**, 4517 (2014).

[19] A. Koseska, E. Volkov, and J. Kurths, Oscillation quenching mechanisms: Amplitude vs oscillation death, Phys. Rep. **531**, 173 (2013).

[20] M. Y. Kim, R. Roy, J. L. Aron, T. W. Carr, and I. B. Schwartz, Scaling Behavior of Laser Population Dynamics with Time-Delayed Coupling: Theory and Experiment, Phys. Rev. Lett. **94**, 088101 (2005).

[21] P. Kumar, A. Prasad, and R. Ghosh, Stable phase-locking of an external-cavity diode laser subjected to external optical injection, J. Phys. B: At., Mol. Opt. Phys. **41**, 135402 (2008).

[22] W. Zou, X. Wang, Q. Zhao, and M. Zhan, Oscillation death in coupled oscillators, Front. Phys. China **4**, 97 (2009).

[23] W. Zou and M. Zhan, Complete synchronization in coupled limit-cycle systems, Europhys. Lett. **81**, 10006 (2008).

[24] H. Nakao and A. S. Mikhailov, Diffusion-induced instability and chaos in random oscillator networks, Phys. Rev. E **79**, 036214 (2009).

[25] Z. Hou and H. Xin, Oscillator death on small-world networks, Phys. Rev. E **68**, 055103(R) (2003).

[26] W. Liu, X. Wang, S. Guan, and C.-H. Lai, Transition to amplitude death in scale-free networks, New J. Phys. **11**, 093016 (2009).

[27] L. M. Pecora and T. L. Carroll, Master Stability Functions for Synchronized Coupled Systems, Phys. Rev. Lett. **80**, 2109 (1998).

[28] R. Grimshaw, *Nonlinear Ordinary Differential Equations* (Blackwell, Oxford, 1990).

[29] W. Magnus, On the exponential solution of differential equations for a linear operator, Commun. Pure Appl. Math. **7**, 649 (1954).

[30] D. J. Watts and S. H. Strogatz, Collective dynamics of 'small world' networks, Nature (London) **393**, 440 (1998).

[31] J. Schnakenberg, Simple chemical reaction systems with limit cycle behavior, J. Theor. Biol. **81**, 389 (1979).